Gelatin-*g*-Poly(methyl methacrylate)/Silver Nanoparticle Hybrid Films and the Evaluation of Their Antibacterial Activity

Ying Liu, Xiaoheng Liu, Xin Wang, Jiazhi Yang, Xu-Jie Yang, Lude Lu

Key Laboratory for Soft Chemistry and Functional Materials, Nanjing University of Science and Technology, Ministry of Education, Nanjing 210094, China

Received 7 May 2009; accepted 2 November 2009
DOI 10.1002/app.31784
Published online 27 January 2010 in Wiley InterScience (www.interscience.wiley.com).

ABSTRACT: We designed and prepared novel hybrid films of nanoparticles consisting of gelatin-*g*-poly(methyl methacrylate) (PMMA)/silver (Ag) polymers with ordered nanoporous, higher antibacterial activities. First, the gelatin-grafted PMMA microspheres were fabricated with the *in situ* copolymerization of gelatin and alkenes under radical initiation, which acted as a stabilizer and regulator for Ag nanoparticle growth. Then, silver nitrate was entrapped in a copolymerization system at 40°C for 30 min. Finally, the gelatin-*g*-PMMA/Ag polymer hybrid films were prepared by the reduction of Ag^+ with hydrazine, followed by emulsion solidification. The antibacterial activities of the gelatin-*g*-PMMA/Ag polymer hybrid films against *Escherichia coli* and *Staphylococcus aureus* were found with the disc diffusion method and colony count assays to be clear and lasting. In this study, our work not only presented a good example of a nanoporous antibacterial film material but also provided a facile method for making use of gelatin and metal/inorganic self-assemble properties in graft copolymerization to prepare functional polymer hybrids, such as antibacterial, antithrombogenic, and dot-quantum effect materials. © 2010 Wiley Periodicals, Inc. J Appl Polym Sci 116: 2617–2625, 2010

Key words: biological applications of polymers; graft copolymers; nanocomposites; self-assembly; thin films

INTRODUCTION

In recent years, ordered porous biopolymer materials have aroused great interest because of their biomedical applications, such as those in tissue engineering, pharmaceutical carriers, and medical devices.[1–6] In the past, a large number of materials, synthetic and natural, have been used to explore porous biomaterials. The most frequently used synthetic porous polymers include poly(glycolic acid),[7,8] poly(D,L-lactic acid),[9,10] and poly(methyl methacrylate) (PMMA).[11–13] Common natural materials include chitosan,[14,15] cellulose,[16,17] and gelatin.[18–20] In this study, gelatin was selected because it is a self-assembling, nontoxic, biodegradable, inexpensive, and nonimmunogenic material. It has been widely applied in medicine for dressing wounds, as an adhesive, and so on. Moreover, gelatin has been proven to form porous materials by the classical synthetic porous polymer materials method, which is based on the use of molecules such as solvents or gases as simple porogens to produce structural pores within the system.[21]

However, one disadvantage of gelatin films is their toughness and brittleness, which originates from their slight swelling in water, and the sol–gel transition temperature of gelatin is approximately 30°C. Because of the suspended double bonds on the side chain in gelatin, one can imagine that one simple way of introducing the gelatin units is through the copolymerization of gelatin and alkenes under radical initiation. For example, the grafting of methyl methacrylate (MMA) species onto gelatin chains to improve gelatin properties has been discussed.[22,23] Furthermore, biomaterials generally require biocompatibility because they are constantly exposed to human fluid environments, such as those in blood and physiological fluids. Therefore, it is both ideal and essential to develop biomaterials that possess not only excellent biocompatibility and long-term stability but also antibacterial functions. The silver (Ag) nanoparticle is a biocompatible metal and is widely used as an antibacterial agent.[24,25] As a

Correspondence to: X. Wang (wxin@public1.ptt.js.cn).
Contract grant sponsor: National Natural Science Foundation of China.
Contract grant sponsor: China Academy of Engineering Physics; contract grant number: 10776014.
Contract grant sponsor: High Technical Foundation of Jiangsu Province of China; contract grant number: BG2007047.

result, films containing gelatin, PMMA, and Ag species would be excellent polymer hybrids with biocompatibility and antibacterial abilities.

In this study, our goal was to design a porous and antibacterial gelatin-grafted PMMA/Ag (gelatin-*g*-PMMA/Ag) polymer nanoparticle hybrid film. We selected MMA grafting gelatin not only to improve the gelatin film adhesion and wetting behavior, as well as avoid dissolution at body temperature (37°C),[26] but also to regulate Ag nanoparticle growth in MMA and gelatin copolymerization nanoemulsion in preparation of a functional gelatin-based biomaterial. To achieve this goal, the gelatin-*g*-PMMA macromolecular compound was synthesized through the copolymerization of gelatin and alkenes under radical initiation. Then, Ag nanoparticles were anchored on the gelatin-*g*-PMMA macromolecules by ligand-stabilizing nanoparticles. The ordered nanoporous film was obtained by gelatin-*g*-PMMA/Ag emulsion solidification. The antibacterial activities of the films to *Escherichia coli* and *Staphylococcus aureus* were evaluated by the disc diffusion method and colony count assays. Consequently, this study not only presented a good example of obtaining a nanoporous antibacterial film material via a facile route but also made full use of gelatin and metal/inorganic self-assemble abilities in copolymerization to prepare functional gelatin-based polymer hybrids.

EXPERIMENTAL

Materials

Gelatin (type B, extracted from bovine skin, molecular weight = 100,000 g/mol) was purchased from Tianjin Kermel Chemical Reagent Co., Ltd. (Tianjin, China). MMA, potassium persulfate ($K_2S_2O_8$), silver nitrate ($AgNO_3$), and hydrazine were obtained from Sinopharm Chemical Reagent Co., Ltd. (Shanghai, China). MMA was washed with 5% aqueous alkaline to remove the phenolic inhibitor and then vacuum-distilled before use. All other chemicals were analytical grade and were used as received.

Synthesis of gelatin-*g*-PMMA

The synthesis of gelatin-*g*-PMMA was performed as described earlier.[22] Gelatin (1.0 g) was dissolved in 50 mL of water and mixed with a purified calculated amount of MMA monomer in a water-jacketed flask equipped with a thermometer, a condenser, a magnetic stirrer, and a nitrogen inlet. The stirred mixture was purged with nitrogen for 30 min. $K_2S_2O_8$ (5×10^{-3} mol) was added, and the mixture was heated at 60°C for 1 h under nitrogen. The gelatin-*g*-PMMA copolymer was separated from PMMA by precipitation of the reaction mixture with acetone, where the PMMA dissolved and the precipitated copolymer was filtered and dried. Finally, the grafted sample was extracted with acetone in a Soxhlet apparatus for 48 h to dissolve all of the homopolymer. The product was dried *in vacuo* at 50°C for 24 h to a constant weight and later characterized by Fourier transform infrared (FTIR) spectroscopy. The MMA conversion was determined gravimetrically. The grafting percentage and grafting efficiency were calculated as follows:

$$\text{Grafting percentage} = \frac{\text{Weight of the grafted PMMA}}{\text{Weight of the gelatin}} \times 100\%$$

$$\text{Grafting efficiency} = \frac{\text{Weight of the grafted PMMA}}{\text{Weight of the total polymerized polymer PMMA}} \times 100\%$$

The water solubility of gelatin-*g*-PMMA was determined as described by Lee et al.[27] The purified gelatin-*g*-PMMA (10 g) was soaked in water (100 g, pH = 7.0 ± 0.2) under vibration at 170 rpm for 48 h at 37°C. Then, the mixture was separated by centrifugation at 2700 rpm for 10 min. We obtained the mass of gelatin-*g*-PMMA dissolved in water by drying the upper liquid *in vacuo* at 50°C for 24 h to a constant and then weighing. The water solubility of gelatin-*g*-PMMA was defined as the mass of gelatin-*g*-PMMA dissolved in 100 g of water at 37°C. Each solubility value was determined at least in triplicate.

Preparation of the gelatin-*g*-PMMA/Ag film

A white emulsion containing the gelatin-*g*-PMMA microspheres was obtained according to the procedure in the Synthesis of Gelatin-*g*-PMMA section. The $AgNO_3$ (5 mL, 0.03*M*) solution was dropped into the emulsion (50 mL) under stirring at 40°C in 10 min. After 0.5 h, a black emulsion was obtained by the reduction of Ag^+ with hydrazine. The gelatin-*g*-PMMA/Ag thin film was prepared by crude product emulsion solidification on a glass plate at room temperature. To remove residual KNO_3 and unreacted gelatin, the crude gelatin-*g*-PMMA/Ag nanocomposite hybrid film was washed with distilled water at 40°C. Then, the thin film was soaked in acetone to remove PMMA homopolymer. Finally, the gelatin-*g*-PMMA/Ag polymer hybrid film was dried for 24 h *in vacuo* at 40°C for succeeding experiments.

Characterization

FTIR spectroscopy

FTIR spectroscopy was used to investigate the structures of the gelatin-*g*-PMMA and gelatin-*g*-PMMA/

Ag films. The spectra were recorded on an Equinox 55 spectrometer (Bruker Co., Germany). Blank scanning was performed before the measurements to eliminate the influence of water vapor and CO_2 in the air.

Transmission electron microscopy (TEM) and scanning electron microscopy (SEM)

Morphological studies of the gelatin-*g*-PMMA/Ag films were carried out with TEM (JEOL JSM-2100, Japan). The gelatin-*g*-PMMA/Ag film sample was broken up and transformed into alcohol. After the film was treated by ultrasonication in alcohol, the sample was dropped onto a carbon-coated copper grid and observed with a JEOL JSM-2100 transmission electron microscope operated at 200 kV, and images were recorded digitally with a Gatan 794 charge-coupled device camera. In SEM (JEOL-6380LV, Japan), we used conventional specimen preparation and imaging techniques.

X-ray powder diffractometry

Powder X-ray diffraction (XRD) patterns of the gelatin-*g*-PMMA/Ag film sample was recorded on a Bruker D8 with Cu Kα radiation (λ = 1.5418 Å) in the range 2.1–60°.

Ultraviolet–visible (UV–vis) spectra

UV–vis absorption spectra of the gelatin-*g*-PMMA and gelatin-*g*-PMMA/Ag hybrid emulsions were obtained on a Rayleigh UV-1201 (Beijing, China) recording spectrophotometer.

Antibacterial evaluation

Zone of inhibition method

The antibacterial activities of gelatin-*g*-PMMA/Ag against *E. coli* and *S. aureus* were evaluated with the disc diffusion method. Nutrient agar plates were prepared by the dissolution of 14 g of agar, 3 g of beef broth, 10 g of protein, and 5 g of NaCl in 1 L of water. The pH of the solution was then adjusted to 7.0 ± 0.2. The contents were then sterilized by autoclaving at 0.1 MPa of pressure for 1 h. The agar was poured into Petri plates in quantities of 15 mL and left on a flat surface to solidify. The bacterial culture was incubated in broth at 37°C for 24 h and diluted to 10^5 cfu/mL. They were then pipetted onto agar plates prepared as described previously.

The gelatin-*g*-PMMA/Ag film was cut into a 9-mm diameter disk. The previously prepared film was applied to the surface of the inoculated agar plates. After 24 h of incubation at 37°C, the plates were examined, and the diameter of the growth inhibition zone around the sample disc was measured.

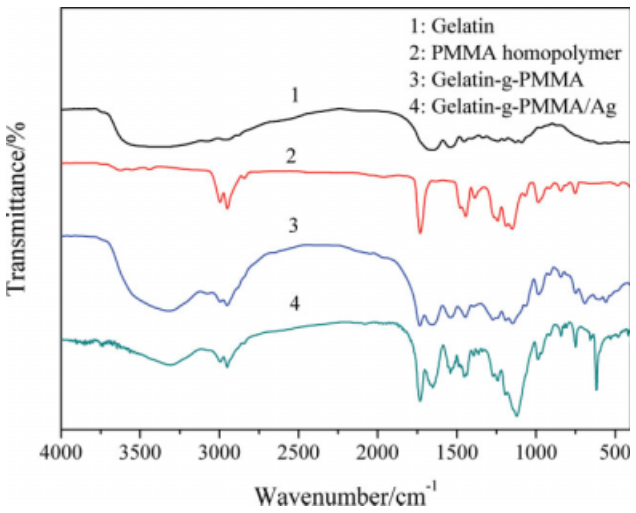

Figure 1 FTIR spectra of the (1) gelatin, (2) PMMA homopolymer, (3) gelatin-*g*-PMMA, and (4) gelatin-*g*-PMMA/Ag. [Color figure can be viewed in the online issue, which is available at www.interscience.wiley.com.]

Colony counting method

The antibacterial activity of gelatin-*g*-PMMA/Ag film against *E. coli* and *S. aureus* was also compared with colony counting. The gelatin-*g*-PMMA/Ag film was crushed into powder. The sample concentrations (50 μg/mL) were evaluated. The bacterial culture was incubated in broth with gelatin-*g*-PMMA/Ag powder for 12 and 24 h at 37°C. Finally, the bacterial liquid was pipetted onto agar plates prepared as described previously. The plates were examined, and the colonies were counted after incubation for 24 h at 37°C.

RESULTS AND DISCUSSION

Characterization of the porous gelatin-*g*-PMMA/Ag film structure

The typical FTIR spectrum of gelatin (curve 1), as shown in Figure 1, displayed bands at 3100–3500 cm^{-1} (N—H stretching), 1647 cm^{-1} (amide carbonyl C—O stretching), 1536 cm^{-1} (N—H bending), 1447 cm^{-1} (C—N stretching), and 647 cm^{-1} (N—H deforming).[28] In contrast, bands corresponding to the C=O and C—O stretching modes appeared at about 1730 and 1150 cm^{-1}, respectively, as well as the band at about 989 cm^{-1} assigned to the C—O—C symmetrical stretching mode of the PMMA chains in the PMMA homopolymer (see curve 2), gelatin-*g*-PMMA (see curve 3), and gelatin-*g*-PMMA/Ag (see curve 4); these indicated the copolymerization of MMA and gelatin. Furthermore, the spectra of

gelatin-*g*-PMMA/Ag showed almost the same bands as gelatin-*g*-PMMA except for a blueshift of 7–30 cm^{-1} and an increase in the band intensity for all peaks. For example, the intensity of the —N—H deforming band of gelatin chains at 647 cm^{-1} for pure gelatin-*g*-PMMA (in the absence of Ag nanoparticles) increased greatly and turned to 619 cm^{-1} in the gelatin-*g*-PMMA/Ag composites. This was possibly because of chemical bonding between the Ag nanoparticles with methionine groups in gelatin[29] and the oxygen atoms of PMMA chains.[30]

The relation between the graft copolymerization and MMA concentration is illustrated in Figure 2. As the monomer reaction probability impacted polymerization, the MMA monomer concentration increase was favorable for the rate of graft copolymerization and MMA homopolymerization. The grafting percentage increased, but the grafting efficiency decreased with increasing mass ratio of MMA to gelatin. Significantly, the PMMA grafted percentage was a key factor in the impact on the antibacterial activity of the gelatin-*g*-PMMA/Ag film. Therefore, a higher percentage of grafted PMMA resulted in poorer wetting behavior in the gelatin-*g*-PMMA/Ag film and thereby would induce tiny interactions between the Ag nanoparticles and bacteria in human fluid environments. Therefore, the antibacterial activity of the gelatin-*g*-PMMA/Ag film was not clear. At the time, a lower PMMA grafted percentage may have caused the gelatin-*g*-PMMA/Ag thin film to dissolve in water at body temperature. The water solubilities of gelatin-*g*-PMMA with different graft percentages at 37°C are shown in Figure 3. In this study, we selected a mass ratio of 1 to carry out the following experiments because of the relatively higher water solubility, grafting efficiency, and percentage (see the Evaluation of the Antibacterial Activity section).

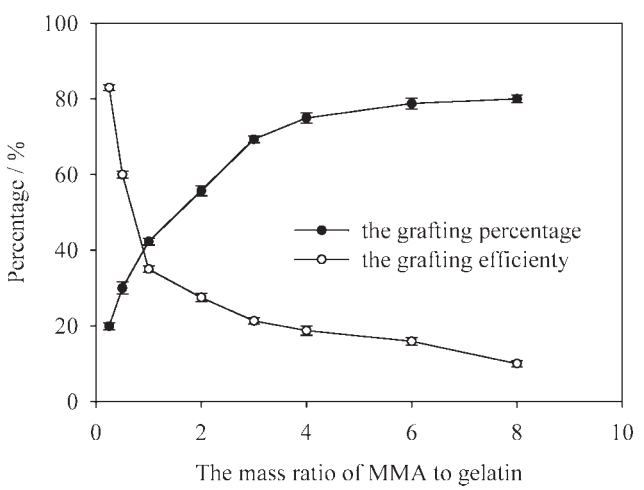

Figure 2 Effect of the MMA concentration on the graft copolymerization of MMA and gelatin (0.01*M* $K_2S_2O_8$). Each data point is the mean of three samples, and error bars are the standard deviations.

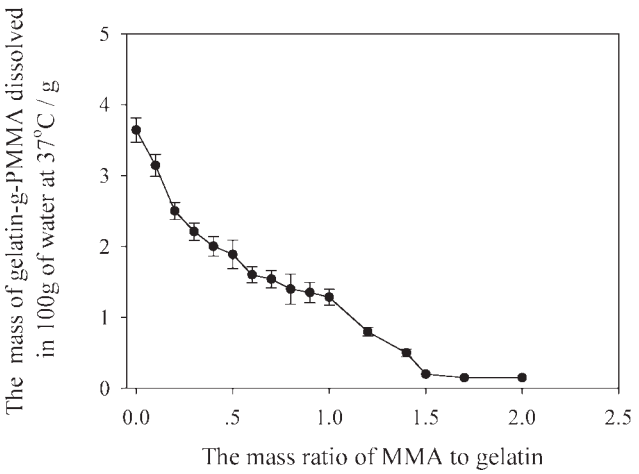

Figure 3 Effect of the MMA concentration in the graft copolymerization on the water solubility of the gelatin-*g*-PMMA copolymer (0.01*M* $K_2S_2O_8$). Each data point is the mean of three samples, and error bars are the standard deviations.

Gelatin, a peptide chain, is an amphiphilic electrolyte with active terminal amino groups and polypeptide linkages. Gelatin has the capability of stabilizing hydrophobic MMA monomer micelles in water. The graft copolymerization of MMA and gelatin and MMA homopolymerization is within an oil-in-water micelle. Li et al.[22] testified that a graft copolymer of MMA and gelatin formed polymer nanospheres with diameters of 80–100 nm by *in situ* copolymerization in water, where PMMA cores were coated with hydrophilic gelatin shells. Inset (a) in Figure 4 shows a digital photograph of the gelatin-*g*-PMMA white emulsion obtained according to the procedure in the Synthesis of Gelatin-*g*-PMMA section; this emulsion was stable in water without sedimentation at room temperature for at least 2 months. Therefore, the gelatin-*g*-PMMA emulsion was a nanoscaled emulsion with great stability, which could be used as template and regulator for the preparation of Ag nanoparticles. The mass ratio of Ag (determined by the amount of $AgNO_3$ added to the reaction mixture) to gelatin ($m_{Ag}/m_{gelatin}$) was 26.5 mg/g in the gelatin-*g*-PMMA/Ag hybrid emulsion obtained according to the procedure in the Preparation of the Gelatin-*g*-PMMA/Ag Film section [see inset (b) in Fig. 4].

The UV–vis spectra of gelatin-*g*-PMMA/Ag showed that the absorbance band at 433 nm was an Ag nanoparticle surface plasmon band via a comparison curve 4 with curve 5 in Figure 4, which was in agreement with a previous article.[31] With decreasing Ag nanoparticle concentration in the emulsion, the Ag nanoparticle surface plasmon band [surface plasmon band maximum (λ_{max}) = 433 nm] remained regularly changeable. This suggested that the Ag

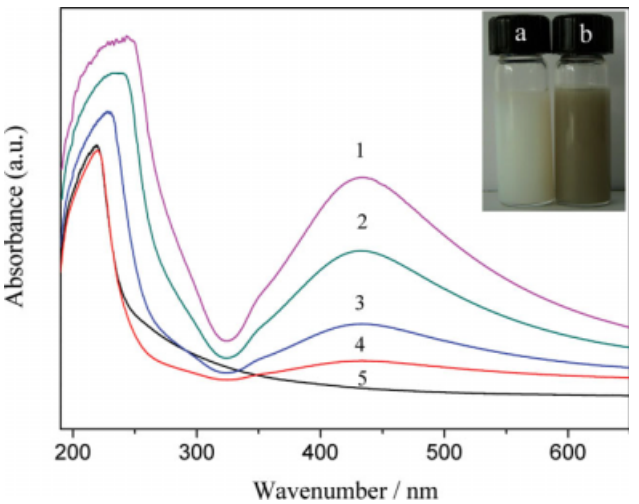

Figure 4 UV–vis spectra of the gelatin-*g*-PMMA/Ag and gelatin-*g*-PMMA emulsion. (1–4): gelatin-*g*-PMMA/Ag emulsion, in which the gelatin concentrations were 0.012, 0.008, 0.004, and 0.002 g/mL, respectively, and (5) gelatin-*g*-PMMA emulsion, in which the gelatin concentration was 0.002 g/mL. Insets (a) and (b) show the emulsion digital photography of the gelatin-*g*-PMMA (white) and gelatin-*g*-PMMA/Ag hybrid emulsion (gray), respectively. [Color figure can be viewed in the online issue, which is available at www.interscience.wiley.com.]

nanoparticles were monodispersed when gelatin-*g*-PMMA was used as a stabilizer. Additionally, with decreasing gelatin concentration in the emulsion, not only did the gelatin-*g*-PMMA absorbance peak (λ_{max}) decrease in intensity, but also the band shift decreased from 240 to 210 nm. The absorption peak position ($\lambda_{max} \approx 230$ nm) excursion of gelatin-*g*-PMMA induced by peptide and PMMA chain conformation changed and decreased in the chemical linkages among the chains in diluted solution, which showed the gelatin peptide and PMMA chain self-assembling abilities in water.[32] The stable Ag nanoparticle surface plasmon band and changeable gelatin-*g*-PMMA band in Figure 4 indicated that the interaction between the gelatin-*g*-PMMA macromolecules and Ag nanoparticle was stable, and the gelatin-*g*-PMMA chain conformation difference and chemical linkage change among the chains had no effect on the Ag particle size. In other words, Ag particles were not simply wrapped among gelatin chains but bound to the gelatin-*g*-PMMA chains in water.

The Ag crystals in the gelatin-*g*-PMMA/Ag film were characterized by XRD (see Fig. 5). The broad peak exhibited at about 14.0° was assigned to reflections from the amorphous copolymer. Peaks at 31.8, 38.2, and 44.3° were attributed to face-centered cubic Ag nanoparticles. The peaks at $2\theta = 38.2$ and 44.3° confirmed the presence of Ag (0) in the sample. The peak at 38.2° with 100% relative intensity peak counts, which confirmed the Ag (0), was same as in JCPDS 04-0783.[33] Furthermore, the peak at 2.9° also suggested that this reflection was from the ordered pore of the gelatin-*g*-PMMA hybrid film. The pore size (d), determined by Bragg's law of diffraction ($2d \sin\theta = n\lambda$; where θ is the scattering angle, n is the order of the diffraction, $n = 1, 2, 3\ldots$), was about 3 nm. As shown in Figure 5, in contrast to the XRD peaks of the copolymer, the XRD peaks of the Ag nanoparticles were not higher; this indicated that gelatin-*g*-PMMA played a significant role in governing the Ag particle growth and crystal growth. The diameter of the gelatin-*g*-PMMA/Ag nanoparticles in the film (L) was estimated according to the Scherrer formula from the full width at half-maximum of the most intense peak (111): $L = 0.9\lambda/\beta \cos\theta_B$, where λ is the wavelength of Cu Kα (1.5406 Å), θ_B is the angle of Bragg diffraction, and $\beta = B - b$ (where B and b represent the full width at half-maximum and the instrumental line broadening, respectively; $b = 0.09$ radian).[34] The crystallite size was calculated to be about 6 nm.

Because of gelatin possesses amphiphilic properties, gelatin peptides in the gelatin-*g*-PMMA copolymer could bind to the Ag nanoparticle surfaces and make the nanoparticles steadily suspendable in water.[35] As a result, the gelatin-*g*-PMMA/Ag/PMMA blend film was uniform by gelatin-*g*-PMMA/Ag emulsion solidification [see Fig. 6(a)]. The gelatin-*g*-PMMA/Ag film, with a wormlike pore structure, was comparatively uniform in width [see Fig. 6(c,d)], which was coincident with the pore size d (3 nm) determined by XRD (see Fig. 5). As the particle size was very small, the Ag particle images in Figure 6(c) are blurry. There was no obvious difference in pore formation between the gelatin-*g*-PMMA film [Fig. 6(b)] and gelatin-*g*-PMMA/Ag film. Therefore, Ag nanoparticles inserted into film did not destroy the structure of the gelatin-*g*-PMMA film.

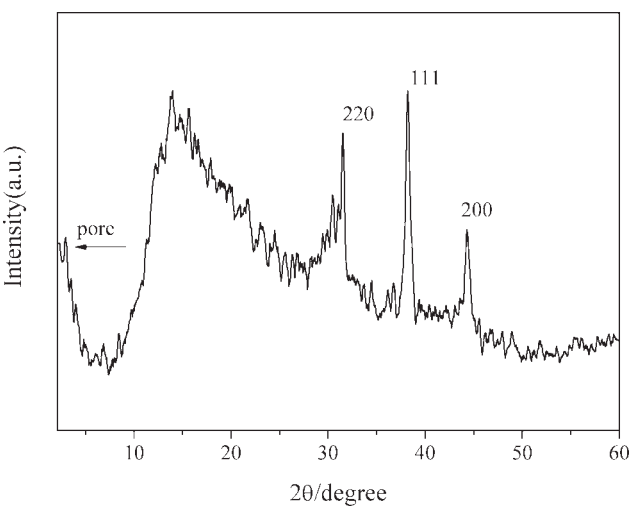

Figure 5 XRD pattern of the gelatin-*g*-PMMA/Ag nanoparticle hybrid film.

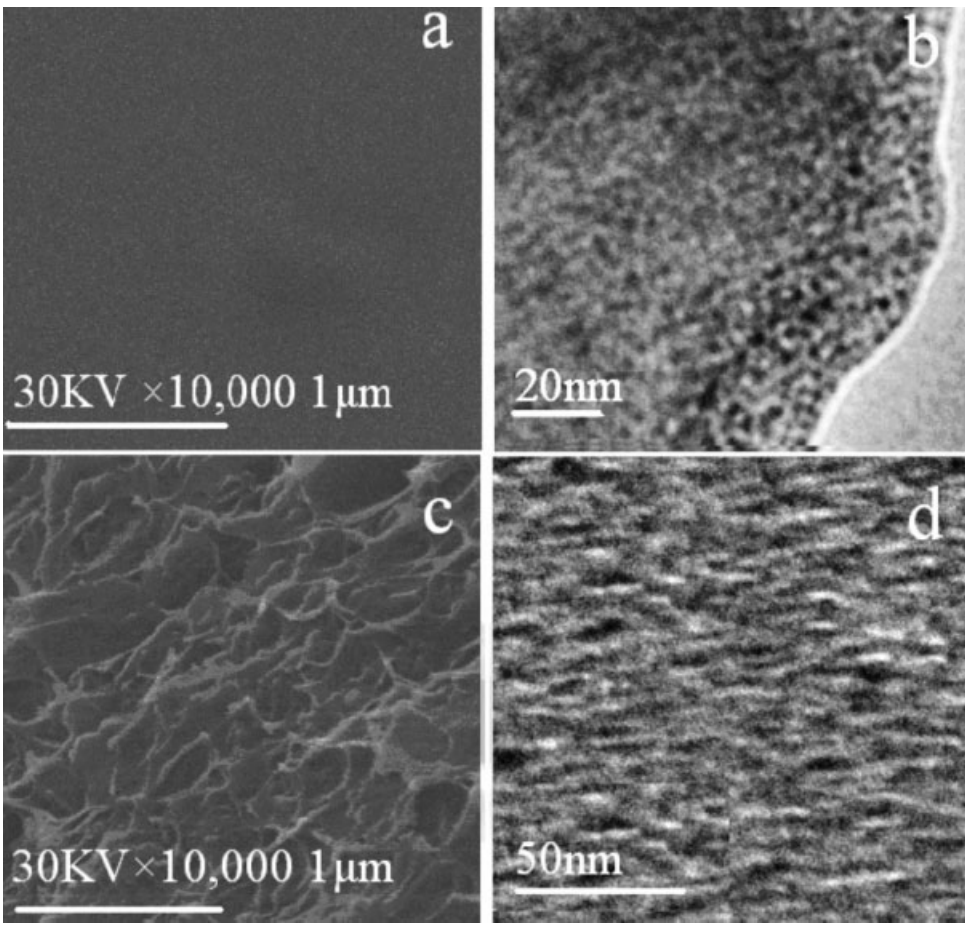

Figure 6 (a) SEM image of the gelatin-*g*-PMMA/Ag/PMMA blend film formed by the solidification of the emulsion obtained according to the procedure described in the Preparation of the Gelatin-*g*-PMMA/Ag Film section at 40°C. (b) TEM image of the gelatin-*g*-PMMA film. (c) SEM image of the gelatin-*g*-PMMA/Ag film. (d) TEM image of the gelatin-*g*-PMMA/Ag film [magnification of Fig. 6(b)].

The pore formation of the gelatin-*g*-PMMA/Ag film, shown in Figure 6, depended on the following aspects: the structure of gelatin and gelatin-*g*-PMMA, the grafting efficiency of PMMA, and acetone volatilization for extraction of gelatin-*g*-PMMA/Ag. First, the architectural parameters of gelatin-*g*-PMMA/Ag, the number of grafts and the distribution of junctions, had effects on the gelatin-*g*-PMMA/Ag film structure. Second, in the drying process of gelatin-*g*-PMMA/Ag, solvent evaporation caused the phase separation of gelatin and PMMA to form a nanopore structure. Finally, during the extraction of gelatin-*g*-PMMA/Ag with acetone, the PMMA homopolymer etched out from the gelatin-*g*-PMMA/Ag bulk may have induced pore formation.

Evaluation of the antibacterial activity

The potential use of gelatin-*g*-PMMA/Ag films as functional biomaterials was assessed by the observation of their antibacterial activities against typical Gram-positive *S. aureus* and Gram-negative *E. coli.* Bacterial liquid without gelatin-*g*-PMMA/Ag was used as a control. The antibacterial activities of gelatin-*g*-PMMA/Ag film against *E. coli* and *S. aureus* were determined with the zone of inhibition method. Sample disks produced a zone of inhibition when they were placed in plates overlaid with *E. coli* or *S. aureus.* The diameters of inhibition for the gelatin-*g*-PMMA/Ag films were 19 and 18.2 mm against *E. coli* and *S. aureus,* respectively (Fig. 7).

The antibacterial activities of gelatin-*g*-PMMA/Ag against *E. coli* and *S. aureus* were also compared with colony counting. A sample concentration of 50 μg/mL was evaluated. Therefore, in this study, the Ag particle concentration in bacteria was evaluated at 1.352 n*M* (determined by the amount of AgNO3 added to the reaction mixture). The results are reported in Figures 8 and 9 and Table I. The gelatin-*g*-PMMA/Ag film showed more than 98% growth inhibition activity on *E. coli* and *S. aureus.* The *E. coli* counts decreased as the time increased from 12 to 24 h. This observation was in accordance with the zone of inhibition data. So, the gelatin-*g*-PMMA/Ag showed clear and durative activity to *E. coli* and *S. aureus.* Also, the inhibitory

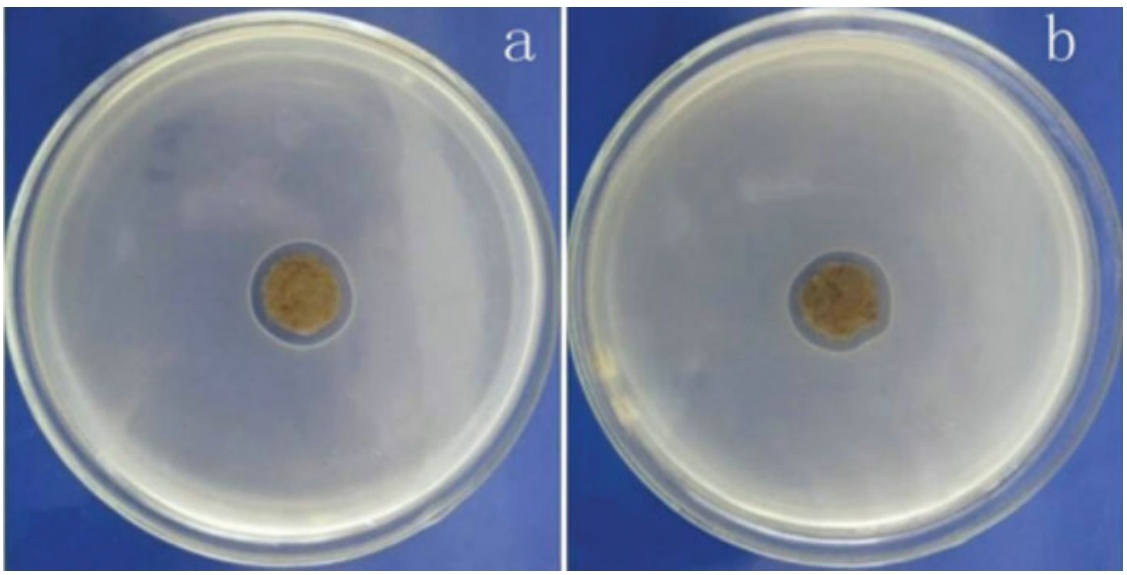

Figure 7 Optical images of the gelatin-*g*-PMMA/Ag film on culture plates inoculated with (a) *E. coli* and (b) *S. aureus*. [Color figure can be viewed in the online issue, which is available at www.interscience.wiley.com.]

concentration of Ag particles in the gelatin-*g*-PMMA/Ag film was far below the minimum inhibitory concentration (3.3–6.6 n*M*) of individual Ag nanoparticles;[24] this probably contributed to the active group of the gelatin peptide chain absorbing ability of the bacterial surface charge to intensify the Ag particle antibacterial activity.

The result of colony counting was clearer than that of the zone of inhibition data. This may have come from the following. It was expected that the wetting behavior of the gelatin-*g*-PMMA/Ag film in the agar (solid state) was much more difficult than in the solution (colony test). There was little chance of the gelatin-*g*-PMMA/Ag film interacting with bacteria. In the colony test, because the gelatin-*g*-PMMA/Ag film could move freely around in the liquid state and be easily wetted and because the porous film possessed a great surface area, many more interactions between the gelatin-*g*-PMMA/Ag powder and bacteria occurred.

Ag nanoparticles show efficient antimicrobial properties compared to other salts because of their extremely large surface area, which provides better contact with microorganisms. The nanoparticles get attached to the cell membrane and also penetrate the bacteria. When Ag nanoparticles enter the bacterial cell, they form a low-molecular-weight region in the center of the bacteria in which the bacteria

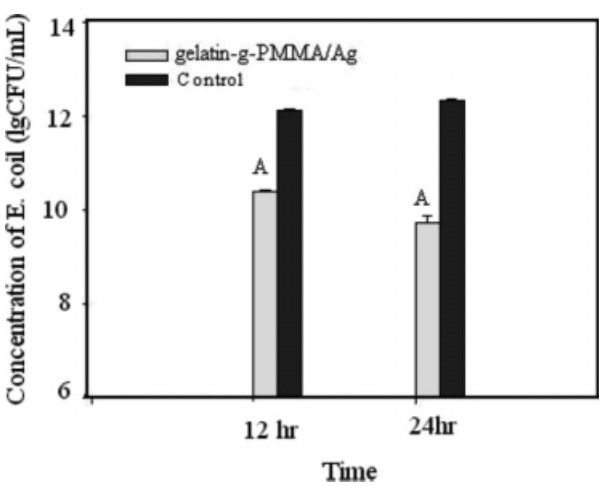

Figure 8 Antibacterial activity of gelatin-*g*-PMMA/Ag at 50 μg/mL against *E. coli* after 12 and 24 h of incubation ($n = 5$, Mean ± Standard deviation). (A) $p < 0.001$ versus control at each time point.

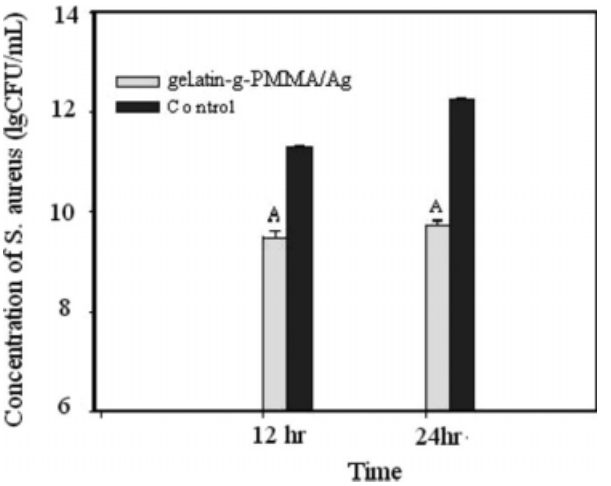

Figure 9 Antibacterial activity of gelatin-*g*-PMMA/Ag at 50 μg/mL to *S. aureus* after 12 and 24 h of incubation. ($n = 5$, Mean ± Standard deviation). (A) $p < 0.001$ versus control at each time point.

TABLE I
Ag Particle Concentration in the Bacteria

	12 h	24 h
E. coli	98.42%	99.61%
S. aureus	98.74%	99.53%

conglomerates; this protects the DNA from the Ag ions. The nanoparticles preferably attack the respiratory chain and cell division; this finally leads to cell death.[36] The nanoparticles release Ag ions in the bacterial cells, which enhance their bactericidal activity.[37] Several possible mechanisms of inhibitory action of Ag on Ag ions (Ag^+) have been discussed in detail in earlier works.[38] Therefore, the antimicrobial effects of Ag nanoparticles depend on characteristics of certain bacterial species and the size of nanoparticles. Gram-positive and Gram-negative bacteria have differences in their membrane structure, the most distinctive of which is the thickness of the peptidoglycan layer.[39] Furthermore, nanoparticles smaller than 10 nm interact with bacteria and produce electronic effects, which enhance the reactivity of the nanoparticles.[40] Because the cell walls of Gram-positive bacteria contain more peptidoglycan layers than those of Gram-negative bacteria, the diameter of inhibition for the gelatin-*g*-PMMA/Ag film against *S. aureus* (a Gram-positive bacterium) was shorter(18.2 mm) than that against *E. coli* (a Gram-negative bacterium), and the *E. coli* counts decreased greatly as time increased form 12 to 24 h. At that time, as the outer thin layer of *E. coli* cells was sensitive to the mechanical power and the bacterial culture was incubated under oscillation as usual, the inhibition activity of gelatin-*g*-PMMA/Ag was clearer at 48 h.

CONCLUSIONS

An ordered, wormlike, porous gelatin-*g*-PMMA/Ag film linked with monodispersed nanoparticles, with higher antibacterial activities against *E. coli* and *S. aureus*, was prepared via a facile route. The Ag nanoparticle concentration in the gelatin-*g*-PMMA/Ag film is 26.5 mg/g ($m_{Ag}/m_{gelatin}$). The size of Ag nanoparticles embedded in the film was about 6 nm, as determined by XRD. The pore size of the gelatin-*g*-PMMA/Ag film was about 3 nm. When we selected the mass ratio of MMA to gelatin as 1 to prepare the gelatin-*g*-PMMA/Ag film with a grafting percentage of 42%, the gelatin-*g*-PMMA/Ag concentration of 50 μg/mL had clear and lasting antibacterial activity. The inhibition efficiency against *E. coli* and *S. aureus* was greater than 98%. Consequently, this composite nanomaterial combined natural/artificial copolymer with metal nanoparticles and is considered to have potential applications in the field of biomaterials in tissue engineering, medical devices, and so on.

The authors thank Hazoor Ahmad Shad, School of Chemistry, University of Manchester, United Kingdom, for his helpful discussion.

References

1. Ma, Z.; Kotaki, M.; Yong, T.; He, W.; Ramakrishna S. Biomaterials 2005, 26, 2527.
2. Kim, I. Y.; Seo, S. J.; Moon, H. S.; Yoo, M. K.; Park, I. Y.; Kim, B. C.; Cho, C. S. Biotechnol Adv 2008, 26, 1.
3. Hoffman, A. S. Adv Drug Delivery Rev 2002, 43, 3.
4. Torchilin, V. P. Adv Drug Delivery Rev 2002, 54, 235.
5. You, B.; Shi, L.; Wen, N.; Liu, X.; Wu, L.; Zi, J. Macromolecules 2008, 41, 6624.
6. Meinel, A. J.; Kubow, K. E.; Klotzsch, E.; Fuentes, M.; Smith, M. L.; Vogel, V.; Merkle, H. P.; Meinel, L. Biomaterials 2009, 30, 3058.
7. Kawanishi, M.; Ushida, T.; Kaneko, T.; Niwa, H.; Fukubayashi, T.; Nakamura, K.; Oda, H.; Tanaka, S.; Tateishi, T. Mater Sci Eng C 2004, 24, 431.
8. Ding, A. G.; Shenderova, A.; Schwendeman, S. P. J Am Chem Soc 2006, 128, 5384.
9. Wang, K.; Thomas, H.; Healy, K. E.; Nuber, G. Polymer 1995, 36, 837.
10. Feng, H.; Dong, C. M. Biomacromolecules 2006, 7, 3069.
11. Singh, N.; Tripathi, D. N.; Tiwari, A.; Sanghi, R. Carbohydr Polym 2006, 65, 35.
12. Pascual, B.; Goñi, I.; Gurruchaga, M. J Biomed Mater Res 1999, 48, 447.
13. Zilberman, M.; Elsner, J. J. J Controlled Release 2008, 130, 202.
14. Prego, C.; Torres, D.; Fernandez-Megia, E.; Novoa-Carballal, R.; Quiñoá, E.; Alonso, M. J. J Controlled Release 2006, 111, 299.
15. Amsden, B. G.; Sukarto, U.; Knight, D. K.; Shapka, S. N. Biomacromolecules 2007, 8, 3758.
16. Liu, W.; Liu, R.; Li, Y.; Kang, H.; Shen, D.; Wu, M. Huang, Y. Polymer 2009, 50, 211.
17. Khan, F. Biomacromolecules 2004, 5, 1078.
18. Griffiths, P. C.; Fallis, I. A.; Teerapornchaisit, P.; Grillo, I. Langmuir 2001, 17, 2594.
19. Ohya, S.; Kidoaki, S.; Matsuda, T. Biomaterials 2005, 26, 3105.
20. Johnson, A. W.; Serrano, N. J.; Morgan, A. W.; Jamison, R.; Choy, Y. B.; Choi, H.; Kim, K.; Decarlo, F. Macromol Symp 2005, 227, 295.
21. Vlierberghe, S. V.; Cnudde, V.; Dubruel, P.; Masschaele, U.; Cosijns, A.; Paepe, I. D.; Jacobs, P. J. S.; Hoorebeke, L. V.; Remon, J. P.; Schacht, E. Biomacromolecules 2007, 8, 331.
22. Li, P.; Zhu, J.; Sunintaboon, P.; Harris, F. W. Langmuir 2002, 18, 8641.
23. Bhattacharya, A.; Misra, B. N. Prog Polym Sci 2004, 29, 767.
24. Jun, S. K.; Kuk, E.; Yu, K. N.; et al. Nanomedicine 2007, 3, 95.
25. Furno, F.; Morley, K. S.; Wong, B.; Sharp, B. L.; Arnold, P. L.; Howdle, S. M.; et al. J Antimicrob Chemother 2004, 54, 1019.
26. Dubruel, P.; Unger, R.; Vlierberghe, S. V.; Cnudde, V.; Jacobs, P. J. S.; Schacht, E.; Kirkpatrick, C. J. Biomacromolecules 2007, 8, 338.
27. Lee, K. Y.; Shim, J.; Lee, H. G. Carbohydr Polym 2004, 56, 251.
28. Lin, L.; Chen, K. J. Colloid Interface Sci A 2006, 272, 8.
29. Kapoor, S.; Lawless, D.; Kennepohl, P.; Meisel, D.; Serpone, N. Langmuir 1994, 10, 3018.
30. Rajendran, S.; Mahendran, O.; Mahalingan, T. Eur Polym J 2002, 38, 45.
31. Thomas, V.; Yallapu, M. M.; Sreedhar, B.; Bajpai, S. K. J Colloid Interface Sci 2007, 315, 89.

32. Bitner, A.; Fiakowski, M.; Smoukov, S. K.; Campbell, C. J.; Grzybowski, B. A. J Am Chem Soc 2005, 127, 6936.
33. Singh, P.; Kumari, K.; Katyal, A.; Kalra, R.; Chandr, R. Spectrochim Acta A 2009, 73, 218.
34. Sertkol, M.; Köseog, Y.; Baykal, A.; Kavas, H.; Basaran, A. C. J Magn Magn Mater 2009, 321, 157.
35. Stanley, B. Nat Biotechnol 1997, 15, 269.
36. Rai, M.; Gade, A. Biotechnol Adv 2009, 27, 76.
37. Morones, J. R.; Elechiguerra, J. L.; Camacho, A.; Ramirez, J. T. Nanotechnol 2005, 16, 2346.
38. Galya, T.; Sedlařík, V.; Kuřítka, I.; Novotoý, R.; Sedlaříkova, J.; Saha, P. J Appl Polym Sci 2008, 110, 3178.
39. Galya, T.; Sedlarik, V.; Kuritka, I.; Sedlarikova, J.; Saha, P. Int J Polym Anal Charact 2008, 13, 241.
40. Raimondi, F.; Scherer, G. G.; Kotz, R.; Wokaun, A. Angew Chem Int Ed 2005, 44, 2190.